Proc. Natl. Acad. Sci. USA
Vol. 96, pp. 7968–7973, July 1999
Cell Biology

p200 ARF–GEP1: A Golgi-localized guanine nucleotide exchange protein whose Sec7 domain is targeted by the drug brefeldin A

SAM J. MANSOUR*†, JENNIFER SKAUG‡, XIN-HUA ZHAO*, JENNIFER GIORDANO*, STEPHEN W. SCHERER‡, AND PAUL MELANÇON*†

*Department of Cell Biology, University of Alberta, MSB 5-14, Edmonton, AB T6G 2H7, Canada; and †Department of Genetics, The Hospital for Sick Children, Toronto, ON M5G 1X8, Canada

Communicated by Randy Schekman, University of California, Berkeley, CA, May 7, 1999 (received for review January 21, 1999)

ABSTRACT **The drug brefeldin A (BFA) disrupts protein traffic and Golgi morphology by blocking activation of ADP ribosylation factors (ARFs) through an unknown mechanism. Here, we investigated the cellular localization and BFA sensitivity of human *p200 ARF-GEP1* (*p200*), a ubiquitously expressed guanine nucleotide exchange factor of the Sec7 domain family. Multiple tagged forms of the full-length polypeptide localized to tight ribbon-like perinuclear structures that overlapped with the Golgi marker mannosidase II and were distinct from the pattern observed with ERGIC53/58. Analysis of several truncated forms mapped the Golgi-localization signal to the N-terminal third of p200. BFA treatment of transiently or stably transfected cells resulted in the redistribution of Golgi markers and in loss of cell viability, thereby indicating that overproduction of p200 may not be sufficient to overcome the toxic effect. A 39-kDa fragment spanning the Sec7 domain catalyzed loading of guanosine 5′-[γ-thio]triphosphate onto class I ARFs and displayed clear sensitivity to BFA. Kinetic analysis established that BFA did not compete with ARF for interaction with p200 but, rather, acted as an uncompetitive inhibitor that only targeted the p200-ARF complex with an inhibition constant of 7 μM. On the basis of these results, we propose that accumulation of an abortive p200-ARF complex in the presence of BFA likely leads to disruption of Golgi morphology. *p200* mapped to chromosome 8q13, 3.56 centirays from WI-6151, and database searches revealed the presence of putative isoforms whose inhibition may account for the effects of BFA on various organelles.**

Treatment of most animal cells with the fungal metabolite brefeldin A (BFA) disrupts protein traffic and leads to morphological reorganization of various organelles (1). This outcome makes BFA a useful agent for exploring mechanisms relevant to organelle biogenesis and membrane dynamics. A block in the assembly of coat proteins on Golgi cisternae represents one of the earliest changes (2) and is apparently a consequence of the inhibition of a Golgi-associated guanine nucleotide exchange factor (GEF) that activates small GTPases of the ADP ribosylation factor (ARF) family (3–5). The identity of the Golgi-specific target remains unknown.

Several mammalian ARF-GEFs have been identified that share a 200-aa domain known as the Sec7 domain. Preliminary analysis of the catalytic mechanism implicated a highly conserved Sec7 domain glutamic acid sidechain that inserts into the GDP binding pocket of ARF and facilitates GDP release before GTP loading (6, 7). Sec7 domain family members can be classified into two subgroups based on size and overall organization. The small molecular weight subgroup is composed of ARNO isoforms 1–3 and products of the pleckstrin-Sec7 domains (PSD) genes. These members range in size from 40–60 kDa and contain a pleckstrin homology domain that assists in membrane recruitment (8–11). In particular, ARNO1 is BFA-resistant and appears to associate primarily with endosomal membranes. Vaughan and colleagues purified from bovine brain extracts a member of the large molecular weight subgroup, p200 ARF-GEP1 (p200), and found that it takes part in a 670-kDa complex and displays greatest sequence similarity to yeast Sec7p (12–14). Biochemical assays with soluble hexahistidine-tagged protein recovered from Sf9 cells confirmed its exchange activity as well as sensitivity to BFA (13). Recently, our group cloned a human cDNA encoding another large molecular weight family member termed GBF1 (207 kDa) that shows significant sequence similarity to two *Saccharomyces cerevisiae* proteins, Gea1p and Gea2p (15, 16), and whose overproduction in BFA-sensitive mammalian cells conferred partial resistance to BFA (S.J.M. and P.M., unpublished observation). p200 appears to be the most plausible candidate mediating some of BFA's toxic effects; however, neither its cellular distribution nor its mechanism of inhibition by BFA have been examined. We address these points in the present report.

MATERIALS AND METHODS

cDNA Cloning and Northern Blot Analysis. The cDNA clone was assembled from two overlapping fragments that spanned bases 1–2789 (expressed sequence tag clone AA121552) and bases 1840–5691. The latter fragment was obtained by PCR from testis cDNA (CLONTECH) by using Pfu DNA polymerase (Stratagene) and primers p200F 5′-GTAAACTATGACTGTGACTTAAATGCAGCCA-3′ and p200R 5′-TACTCGGCCGTCATCATTGCTTGTTTATTCCAAGTTCCTG-3′. These fragments were joined via a unique *Spe*I site (position 1884) within the overlap region. To obtain the 3′ untranslated region sequence, a polyadenylated fragment covering bases 4599–6259 was isolated by screening a λ gt10 human pancreatic library (CLONTECH). No attempt was made to join this fragment with the ORF. The library screen yielded another polyadenylated clone that extended ≈2.2 kilobases (kb) beyond base 4830, corresponding to a cDNA of ≈7 kb. Partial sequencing of its downstream end revealed identity with the cow orthologue, with the exception of nine additional nucleotides in the human cDNA. The nucleotide sequence of bases 1–122 was obtained from GenBank accession no. AA121552.

mRNA blots (CLONTECH) were processed at 42°C according to manufacturer's instructions (5 Prime → 3 Prime). Membranes then were washed several times at high stringency [0.1× standard

The publication costs of this article were defrayed in part by page charge payment. This article must therefore be hereby marked "*advertisement*" in accordance with 18 U.S.C. §1734 solely to indicate this fact.

PNAS is available online at www.pnas.org.

Abbreviations: BFA, brefeldin A; GEF, guanine nucleotide exchange factor; ARF, ADP ribosylation factor; kb, kilobase; HA, hemagglutinin; [^{35}S]GTP[γS], 5′-[γ-thio]triphosphate.

Data deposition: The sequence reported in this paper has been deposited in the GenBank database (accession no. AF111162).

†To whom reprint requests should be addressed.

saline citrate (SSC)/0.1% SDS; 65°C] before autoradiography. The actin DNA fragment was obtained from CLONTECH.

Eukaryotic Expression Constructs and Western Blot Analysis. The coding region of p200, starting from the second codon, was subcloned into a modified version of vector pCEP4 (Invitrogen) that yields fusion proteins with a hemagglutinin tag (MA*YPYDVPDYA*SGT; italicized residues) at the N terminus. Five additional constructs were generated that direct the synthesis of five similarly hemagglutinin (HA) -tagged deletion fragments covering amino acids 2–559, 2–890, 560-1849, 891-1849, and 560–890. 293 HEK-EBNA cells were transfected with 0.5 μg of vector DNA by using Lipofectamine (GIBCO/BRL), and then cells were selected in the presence of 0.3 mg/ml hygromycin, and detergent extracts were recovered in 50 mM Tris (pH 8.0), 0.15 M NaCl, 1% Tween-20, and protease inhibitors. Extracts from stably transfected cells were separated by 3.5/8% SDS/PAGE, were transferred to nitrocellulose membrane, and then were probed with antibody 12CA5 and were visualized by horseradish peroxidase-coupled signal detection.

Transient Expression in BHK21 Cells and Immunofluorescence Analysis. BHK21 cells were transfected on coverslips by using Lipofectamine or Fugene 6 (Boehringer Mannheim) and were processed for immunodetection 14–24 hr later. In brief, cells were fixed for 20 min at room temperature in 4% paraformaldehyde/PBS, were permeabilized for 5 min with PBS and 0.1% Tx-100, and then were washed and blocked with PBS, 0.2% gelatin, and 0.05% NaN_3. Incubations with antibodies were performed for 1–1.5 hr at room temperature in PBS and 0.2% gelatin. Mounted coverslips were viewed with an Axioskop (Zeiss), and images were captured with a Spot 1.1 digital camera (Diagnostic Instruments, Sterling Heights, MI). Sources of antibodies were anti-HA (12CA5 or 3F10; Boehringer Mannheim); Texas Red-coupled donkey anti-rabbit IgG and FITC-coupled donkey anti-mouse and goat anti-rat IgGs (Jackson ImmunoResearch); anti-ERGIC53/58 (Molly 6; a generous gift of J. Saraste, Univ. of Bergen); and anti-mannosidase II (K. Moremen, University of Georgia, Athens, GA).

Production of M1 Recombinant Protein in *Escherichia coli*. The DNA region encoding amino acids 560–890 was amplified by PCR with Pfu DNA polymerase and primers p200F2 (5′-GTTGAGATCTGCTAGCCAGAGTGTAGTGGATATTTATGTAAACTATGACTGTGACTTAAATGC-3′) and p200R2 (5′-CTTCCTCGAGTTATCATAGTTCTTTTGTTTCTTTCATTGATATCTTTTTCCCAGCT-3′), yielding an ≈1-kb fragment that was digested with *Nhe*I/*Xho*I and was subcloned into pRSET-A (Invitrogen). The recombinant protein contained a hexahistidine tag (MRGSHHHHHHGMAS) at the N terminus. Its synthesis was induced in BL21DE3 pLysS cells (OD_{600} = 0.6) grown in Luria–Broth medium with addition of 0.4 mM isopropyl β-D-thiogalactoside and further culture for 3 hr at 30°C. Cells from 750-ml cultures were recovered by centrifugation (12,000 × *g* for 2 min at 4°C), were resuspended with 25 ml of 20 mM Tris (pH 8.0) and 0.3 M NaCl, and then were lysed at 4°C with four 30-sec sonication pulses. After clearing (30,000 × *g* for 30 min at 4°C), the supernatant was prepared for chromatography by addition of 5 mM $MgCl_2$, 1 mM EDTA, and 1 mM imidazole. Extracts were incubated with Ni–nitrilotriacetic acid beads (1 ml bed volume; Qiagen, Chatsworth, CA) for 2 hr at 4°C before transfer into a 3-ml column. After a wash with 20 mM Tris (pH 8.0), 0.3 M NaCl, and 40 mM imidazole, bound protein was eluted with 10 ml of 0.25 M imidazole, 25 mM Hepes (pH 7.4), 0.1 M NaCl, 5 mM $MgCl_2$, 1 mM EDTA, and 10% glycerol. Fractions containing recombinant protein (≈9 ml) were pooled and dialyzed against elution buffer lacking imidazole. This preparation yielded ≈70% pure recombinant protein (≈0.16 mg/ml) as judged by SDS/PAGE and Coomassie blue staining.

Guanine Nucleotide Exchange Assays. Reactions were performed at 37°C as described by Frank *et al.* (17) in the presence of 1 μM bovine ARF1 and ARF3, 10–20 nM p200 (M1 fragment), 50 mM Hepes (pH 7.5), 100 mM KCl, 1 mM $MgCl_2$, 1 mM DTT, 1.5 mg/ml azolectin vesicles (Sigma; P-5638), 4 μM 5′-[γ-thio]triphosphate ([^{35}S]GTP[γS]) (3 × 10^5 cpm/pmol; NEN), and either DMSO (final concentration 2.5%) or the indicated concentrations of BFA dissolved in DMSO. Reactions (20 μl) were terminated by diluting with 2 ml of ice-cold wash buffer (50 mM Hepes, pH 7.5/100 mM KCl/10 mM $MgCl_2$). Bound ARF-GTP[γS] was quantified by filtering samples through 0.45 μm nitrocellulose membranes (Millipore, HAWP02400), followed by a rinse with four 2-ml aliquots of wash buffer. Dried filters in 3 ml of liquid scintillant (CytoScint, ICN, San Diego) were analyzed in a 1209 Rack-Beta counter (Amersham Pharmacia). The amount of GTP loaded on ARFs was calculated after subtracting background measured in assays containing only azolectin vesicles and ARF. Background from purified M1 was negligible. IC_{50} values were extrapolated from Dixon plots (1/v vs. [I]) of the kinetic data, excluding unreliable data points showing >90% inhibition. The K_I for BFA was obtained by extrapolating plots of IC_{50} vs. 1/[ARF] to infinite substrate concentration (18).

Genomic Mapping. The NIGMS human rodent somatic cell hybrid mapping panel (no. 2) and the GeneBridge 4 radiation hybrid panel were screened by PCR with a set of primers (5′-ATTTTTGTTGGCATTTACATCCCTCTGCTCTTTA-3′ and 5′-AGACAGGGAAGGACCCGTGAGCATGA-3′) specific for the 3′ untranslated region of the human sequence. A 249-bp product was obtained under the following conditions: initial denaturation for 2 min at 94°C, followed by denaturation for 45 sec at 94°C, annealing for 45 sec at 61°C, and extension for 60 sec at 72°C, for 35 cycles. Further PCR screening of 13 yeast artificial chromosomes from the 8q13 region (718h1, 758b5, 786h12, 810f4, 820e6, 847b11, 876d10, 905c5, 910f5, 925d9, 928f9, 944c9, and 953h7) identified one positive clone, 925d9. The chromosomal assignment was confirmed by the fluorescence *in situ* hybridization mapping method (19) by using bacterial artificial chromosome clone HRG2009J16, whose available sequence from one end displayed 100% identity with cDNA bases 4961–5058.

RESULTS

Human p200 Is Expressed Ubiquitously. The cDNA sequence of human *p200* was assembled from three fragments isolated by PCR and library screens as described in *Materials and Methods* (GenBank accession no. AF111162). The deduced polypeptide of 1,849 amino acids (208.8 kDa) displayed an abundance of acidic residues (pI = 5.67) and shared 98.4% sequence identity with its bovine orthologue. Both of these proteins showed greatest similarity to Sec7p from *S. cerevisiae* (14). Database searches with the compiled sequence revealed the presence of several human expressed sequence tags with minor sequence variation that may correspond to one or several closely related isoform(s) (Table 1). The search also identified a completely sequenced *Drosophila* homologue that mapped nearby *Son of Sevenless*. No reports existed on mutations within this gene.

The expression pattern of the human gene was examined by probing Northern blots with a fragment covering the 5′ untranslated region and the complete ORF. A predominant transcript (≈7.5 kb) along with a minor one (≈7 kb) was observed in various endocrine tissues, particularly in the testis (Fig. 1). A similar pattern of moderate expression also was seen in different regions of the brain (Fig. 1) and in eight cell lines (data not shown). This pattern resembled that previously reported for human *GBF1* (15).

p200 Localizes to Golgi Cisternae. To determine the cellular distribution of p200, we chose to localize epitope-tagged

Table 1. Sequences in the expressed sequence tag database possibly belonging to p200 isoforms*

GenBank accession no.†	Amino acid residues in p200	Segment length, amino acids	No. of matching amino acids	Percent identity
aa399434, aa508649	122–203	82	76	92.7
aa748620	427–567	141	127	90.1
ai380627‡	709–885	177	160	90.4
aa972301	1142–1198	57	52	91.2
w28062	1324–1403	80	72	90.0
x85714	1793–1841	49	40	81.6

*The query sequence covered both the ORF and untranslated regions of human *p200*.
†All human ESTs.
‡Sequence spans the Sec7 domain region.

protein because our attempts to produce antisera were unsuccessful. Several tagged forms were constructed that contained either a hemagglutinin tag (YPYDVPDYA) at the N terminus or a VSV-G tag (TDIEMNRLGK) at the N or C terminus. Western blot analysis of extracts prepared from 293-HEK cells transfected with these constructs confirmed expression of the full-length protein (Fig. 2*A*; data not shown). Transient transfection of flat adherent cells such as BHK21 and NRK cells, followed by indirect immunofluorescence, established that all full-length tagged proteins were targeted to the Golgi apparatus (Fig. 2*B*, left column). Costaining with an antibody that recognizes mannosidase II, a transmembrane Golgi marker, confirmed the assignment (Fig. 2*B*, top row). The tight ribbon-like cisternal localization of p200 was clearly distinct from the more punctate distribution of ERGIC53/58 (Fig. 2*B*, bottom row), a marker of the intermediate compartment between endoplasmic reticulum and Golgi (ERGIC). Analysis of five truncations of p200 demonstrated that Golgi localization signals mapped in the N-terminal third of the protein (Fig. 3).

To examine the consequences of p200 overexpression, we added 0.35 μM BFA to cultures of 293-HEK cells stably producing the full-length protein. Cells stopped growing and died within 1–3 days in a fashion similar to control untransfected ones. In addition, BFA treatment provoked the redistribution of both mannosidase II and p200 in all transiently transfected BHK21 cells, irrespective of expression level (Fig. 2*B*, middle row). The extent of protein overproduction achieved here was insufficient to overcome the action of BFA.

BFA Blocks the ARF-GEF Activity of the Sec7 Domain of p200. The localization of p200 to the Golgi apparatus suggested its involvement in BFA effects on protein traffic, which prompted us to delineate the BFA-sensitive domain and to characterize the inhibition mechanism. Attempts to produce in *E. coli* the full-length protein and two deletion fragments that included the Sec7 domain and either the N-terminal or C-terminal half of the polypeptide did not yield detectable protein. In contrast, a deletion fragment (M1) of 39 kDa was produced in good amounts and yielded a protein with activity. Its boundaries were selected on the basis of our experience with numerous GBF1 deletion fragments and, significantly, the presence of a shared sequence motif lying outside of the Sec7 domain in several large molecular weight family members, including p200, GBF1, Sec7, and EMB30 (Fig. 4 *A* and *B*). We

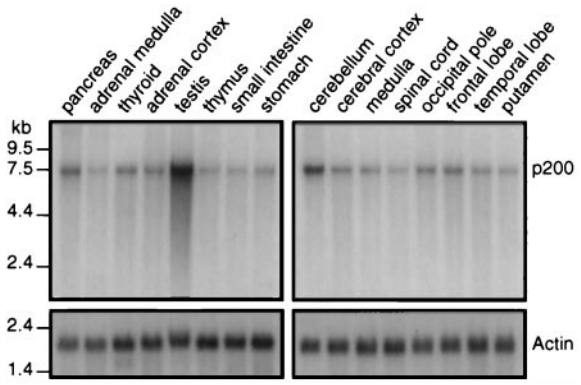

FIG. 1. p200 is ubiquitously expressed in human tissues. mRNA blots were probed with full-length p200 (*Upper*), were washed at high stringency, and then were visualized by autoradiography. The same blots were stripped and reprobed with actin (*Lower*). A minor, 7-kb transcript can be detected in the testes sample at lower exposure.

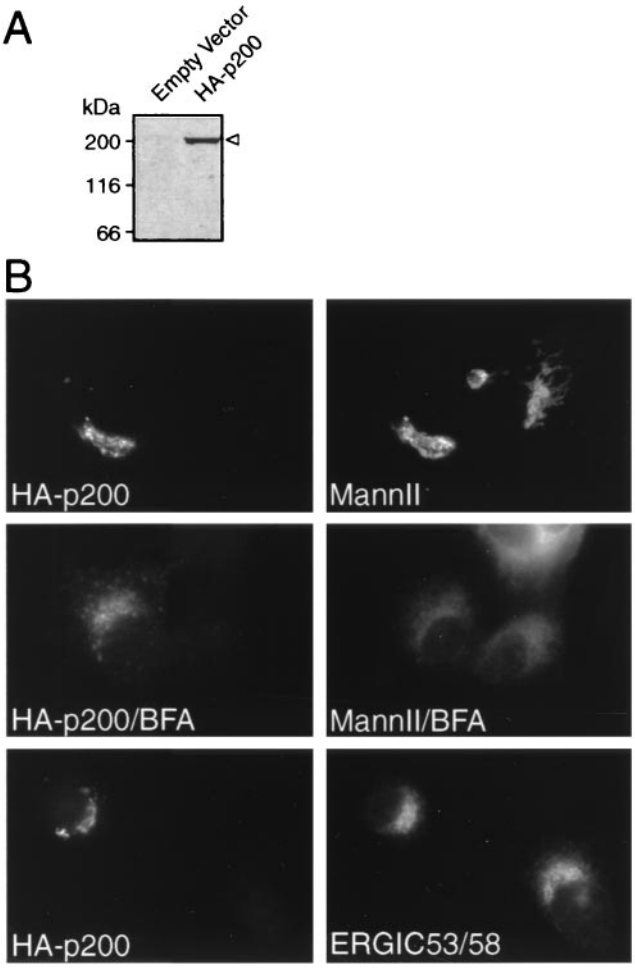

FIG. 2. p200 associates with the Golgi apparatus. (*A*) Production of full-length HA-p200 in 293 HEK-EBNA cells. Detergent extract (60 μg) from stably transfected cells were analyzed by Western blotting to detect HA-tagged p200 (arrowhead). (*B*) Indirect immunofluorescence. BHK21 cells were transiently transfected with the construct encoding HA-tagged protein by using Lipofectamine and were processed for immunofluorescence by using antibodies against the HA epitope (12CA5) and either mannosidase II or ERGIC53/58, as indicated. Each horizontal pair of panels corresponds to a field of view seen with different filters. The distribution of HA-p200 and mannosidase II in cells exposed to 3.5 μM BFA for 10 min before fixation is shown in the middle panels.

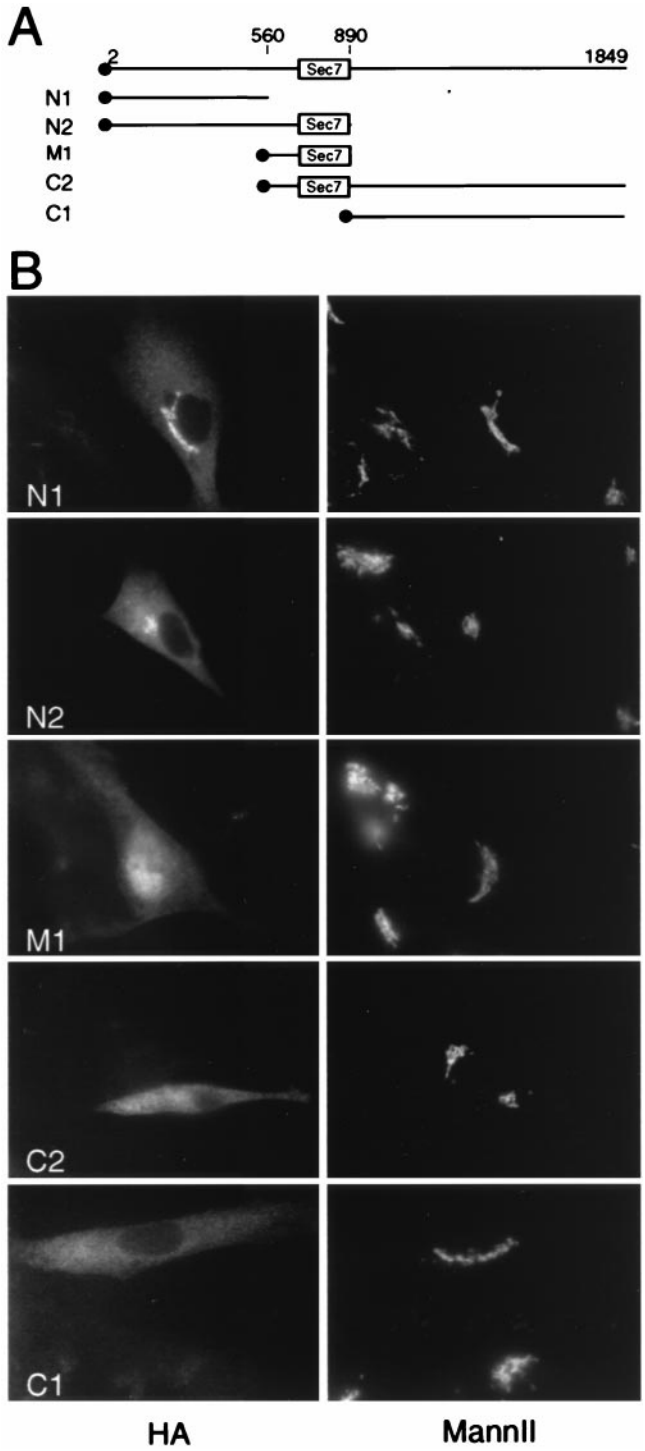

FIG. 3. Localization signal maps to the N-terminal domain. (*A*) Schematic representation of HA-tagged truncations in reference to full-length protein. Numbers refer to the position of amino acids in the full-length polypeptide; the full circle symbolizes the HA tag. (*B*) Indirect immunofluorescence. BHK21 cells were transiently transfected with constructs encoding HA-tagged truncations by using Fugene 6 and were processed for immunofluorescence by using antibodies against the HA epitope (3F10) and mannosidase II. M1, in contrast to other truncations, was not excluded from the nucleus. Each horizontal pair of panels corresponds to a field of view seen with different filters. These results were reproduced in several independent transfections.

propose to name this motif the homology upstream of Sec7 (HUS) box. Its exact role has yet to be explored; however, we speculate that it may be required for protein folding and thermostability.

The guanine nucleotide exchange activity toward a mixture of bovine brain ARF1 and ARF3 was examined by using a relatively pure preparation of M1 (Fig. 4*C*). The loading of GTP[γS] was greatly enhanced at 50:1 substrate:enzyme ratio and was clearly inhibited by addition of 300 μM BFA (Fig. 4*D*). Furthermore, titration with BFA from 25–900 μM in reactions containing 1 μM ARF led to a gradual decrease in nucleotide exchange with an IC_{50} of 125 μM (Fig. 4*E*, middle curve). This effect on a reaction catalyzed by a recombinant protein containing conserved sequence motifs represents the clearest evidence to date that assigns a BFA target.

BFA Targets the Sec7 domain•ARF Complex. To investigate the mechanism of inhibition, we repeated the BFA titrations at various substrate concentrations. At all drug concentrations, raising substrate levels caused an increase in the extent of inhibition (Fig. 4*E*). This result demonstrates that BFA does not prevent substrate binding to the enzyme, thereby excluding a competitive mode of inhibition. To distinguish between other inhibition mechanisms, the readouts of similar kinetic experiments performed over a narrower range of drug concentration were analyzed by using Dixon plots. This analysis yielded parallel lines (Fig. 4*F*), a distinguishing feature of an uncompetitive inhibitor that is only capable of binding the enzyme–substrate complex (18). BFA therefore associates with the p200-ARF1 complex and obstructs further steps during catalysis. Replotting IC_{50} values observed in several experiments (absolute value of x intercept from Dixon plots) as a function of the inverse ARF concentration yielded an inhibition constant (K_I) of 7 ± 3 μM (Fig. 4*G*).

p200 Maps to 8q13. The BFA sensitivity and Golgi localization of p200 suggest this gene plays a key role in protein traffic and may potentially be mutated in pathologies linked to an abnormal protein secretion. As a first step toward molecular characterization of affected loci, we mapped the gene by three complementary methods. PCR screening of cell and radiation hybrid panels localized p200 to chromosome 8q13, 3.56 centirays from WI-6151 (Fig. 5; also see *Materials and Methods*). Further screening of yeast artificial chromosomes in this region identified one positive clone, 925d9. Finally, fluorescence *in situ* hybridization mapping with a bacterial artificial chromosome clone containing p200 sequence confirmed assignment to 8q13. This result added a novel entry to the human gene map according to the latest compilation (20).

DISCUSSION

There has been considerable interest in identifying BFA targets in mammalian cells and in deciphering how inhibition of a subset of these molecules provokes disassembly of the Golgi apparatus. Here, we addressed two outstanding questions pertaining to the functional significance of p200. First, we localized the full-length protein to the Golgi apparatus in transfected cultured cells and mapped the localization signal to amino-terminal third of the protein. Although the purification of bovine p200 from cytosol appears to contradict our immunocytochemical findings, preliminary results with tagged forms of the human protein revealed its presence in both the cytosolic and pelleted membrane fractions of postnuclear supernatants. This finding is consistent with the behavior of numerous transport components that cycle between cytosol and membranes, including *N*-ethyl maleimide-sensitive fusion protein, ARFs, and coatomer. Second, we examined the BFA sensitivity of p200 by using an active fragment produced in bacteria and an assay that measured directly the loading of GTP[γS] onto myristoylated ARF1 and ARF3. This analysis confirmed that the Sec7 domain itself was responsible for BFA sensitivity and allowed us to probe the mechanism of inhibition and establish that BFA does not prevent interaction between ARF and the GEF but, rather, blocks exchange by binding the substrate–enzyme complex as an uncompetitive inhibitor. A

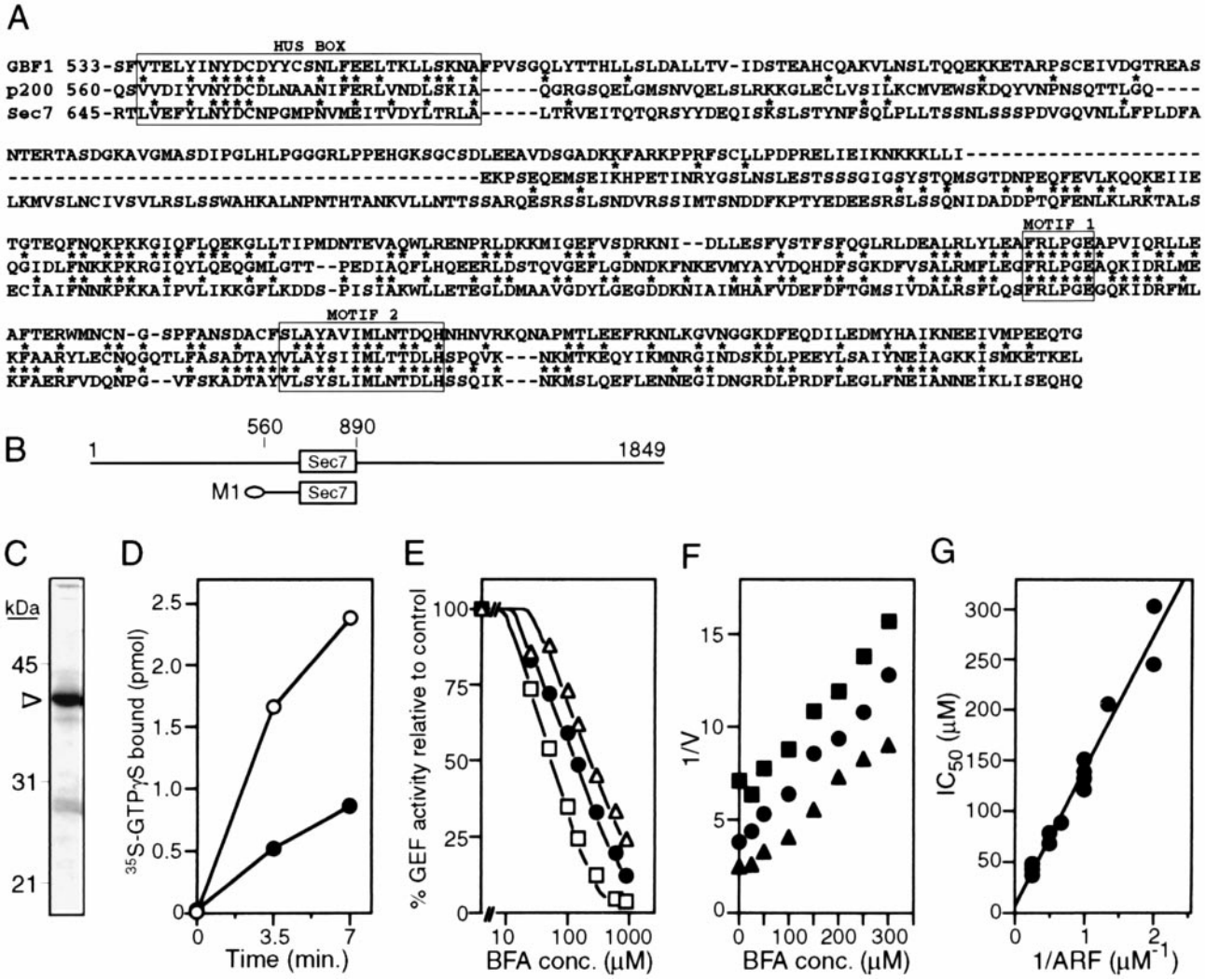

FIG. 4. Guanine nucleotide exchange activity of fragment M1. (*A*) Amino acid sequence alignment of the region extending from the homology upstream of Sec7 box to the end of the Sec7 domain. *, identical residues on pairwise comparison between human p200 and either human GBF1 or yeast Sec7p. The Sec7 domain corresponds to the bottom half of the sequence. (*B*) Schematic representation of fragment M1 in reference to full-length protein. The ellipse at the left side symbolizes the N-terminal hexahistidine tag. (*C*) Partial purification of M1. Dialyzed sample (1 μg) was resolved by SDS/PAGE and was visualized with Coomassie staining. The arrowhead marks the 39-kDa M1 protein. (*D*) Exchange activity toward a mixture of bovine ARF1 and ARF3. Assays were performed in the presence of 1 μM ARF and 20 nM M1, as described in *Materials and Methods*. Open circles, no BFA; filled circles, 300 μM BFA. (*E*) BFA titration at three different ARF concentrations. The exchange rate after 8 min at the indicated BFA concentrations (0, 25, 50, 100, 150, 300, 600, and 900 μM) was measured as in *D* in the presence of 0.5 μM (△), 1 μM (●), or 4 μM (□) ARF, with the exception that the concentration of M1 was reduced to 10 nM. Results are expressed as percent of value measured in absence of BFA for each ARF concentration. Similar IC_{50} values were obtained with 4-min reactions. (*F*) Dixon plots [1/v vs. (BFA)] of BFA titrations. The extent of exchange after 2 min at the indicated BFA concentrations (0, 25, 50, 100, 150, 200, 250, and 300 μM) was measured in duplicate as in *D*. Results with three ARF concentrations are shown: 0.75 μM (■), 1 μM (●), and 1.5 μM (▲). This result was reproduced three times. (*G*) Determination of K_I. IC_{50} values were estimated from Dixon plots of several independent measurements as described in *Materials and Methods* and were replotted as a function of the inverse ARF concentration.

similar result was recently reported (21). The observed fragmentation of the Golgi apparatus on BFA challenge further suggests that formation of the abortive complexes may lead to inhibition of ARF-dependent reactions relevant to maintaining the structural integrity of this organelle.

Our results provided a definitive demonstration of a Golgi-localized BFA target. Previous work with full-length bovine p200 did not address its association with the Golgi apparatus (12, 13). In addition, many of the studies with other ARF-GEFs had either not identified the BFA-sensitive subunit or used experimental conditions for testing BFA sensitivity that were not physiological. For instance, characterization of a partially BFA-sensitive ARF-GEF activity present in a 500- to 600-kDa complex containing Gea1p, a Sec7 domain family member in *S. cerevisiae*, did not identity the susceptible subunit in the complex (16). Recent findings with a truncated recombinant form of the Sec7 domain of yeast Sec7p revealed that its exchange activity displayed varying degrees of BFA sensitivity when assayed at 4–30°C with nonmyristoylated yARFs (22). We and others obtained similar results in assays performed at 30°C by using myristoylated yARF2 (ref. 23; S.J.M. and P.M., unpublished results). In all cases, the truncated forms showed poor catalytic activity and necessitated equimolar amounts of enzyme and substrate (1 μM) (ref. 22; S.J.M. and P.M., unpublished results). The higher specific activity of M1 compared with the yeast Sec7 domain fragment and our ability to monitor BFA sensitivity under more physiological temperature conditions (37°C) and enzyme:substrate ratio (1:100) may have resulted from the inclusion of the homology upstream of Sec7 box found near the N terminus.

The dependence of BFA inhibition on ARF concentration (Fig. 4) provides an explanation for the discrepancy observed

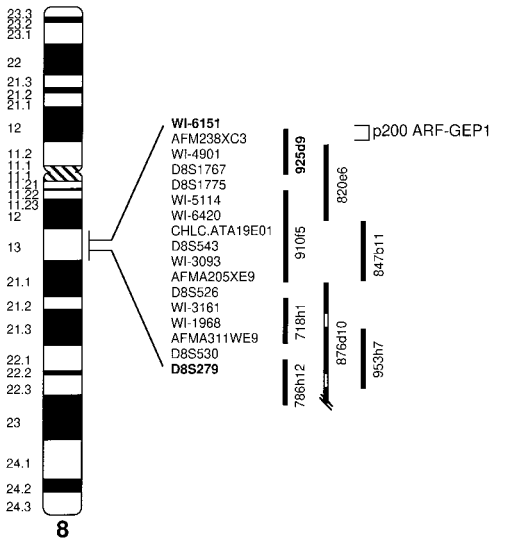

FIG. 5. p200 maps to chromosome 8q13. Yeast artificial chromosomes (vertical bars) covering the 8q13 region were screened by PCR for the presence of p200. Only 925d9 scored positive.

between the levels of BFA needed to inhibit the ARF-GEF activity of purified proteins (Fig. 4; ref. 13) and those needed to inhibit the growth of susceptible cells (IC_{50} of 0.2–0.7 μM) (24, 25) or the ARF-GEF activity of Golgi membranes (IC_{50} of 2–10 μM) (3–5). For example, greater sensitivity in the latter assays could be attributed to high cellular ARF concentration. Alternatively, formation of a ternary complex with ARFs may occur more readily under physiological conditions at which full-length p200 is part of a 670-kDa complex. Furthermore, as discussed below, mammalian cells may contain other BFA-sensitive targets that are affected at lower doses and whose concerted inhibition leads to a compounded response.

Imaging of protein traffic in living cells established that cargo exiting the endoplasmic reticulum first appears in pleiomorphic structures. Subsequent movement of these structures along microtubules toward the Golgi complex (26) is thought to be accompanied by maturation through retrograde traffic of escaped endoplasmic reticulum resident proteins. Both forward movement of cargo to Golgi cisternae and retrieval of endoplasmic reticulum proteins appear to involve the coatomer coat (27) and must require activation of ARFs by specific GEFs. The observation that p200 overlapped significantly with the Golgi marker mannosidase II but showed a distribution clearly distinct from that of ERGIC53/58 suggests that it acts later in this chain of events. However, it is possible that p200 also functions in ERGIC and that its transitory presence is not detectable at steady-state under our experimental conditions.

Previous work with BFA-resistant Chinese hamster ovary cells suggested the presence of multiple organelle-specific targets for BFA that would explain the effects this drug exerts on several organelles of the central vacuolar system (24, 25). For example, the Golgi apparatus in BFY1 cells became highly resistant to BFA whereas the endosomal compartment retained the sensitivity of the parental Chinese hamster ovary line (24). Database searches with the assembled human sequence identified several expressed sequence tags covering multiple regions of sequence identity that may correspond to one or several p200 isoform(s) (Table 1). These candidate molecules, including GBF1 isoforms, represent potential additional targets that could localize to various other organelles or have specialized functions within a particular one.

Our findings set the stage for future work on the recruitment of p200 to Golgi membranes and on the regulation of this process by post-translational modifications during different phases of the cell cycle, particularly on entry into mitosis, when the Golgi disassembles and resident proteins appear to transiently redistribute to the endoplasmic reticulum. Furthermore, the observation that BFA exerts its effects by targeting the p200-ARF complex reveals an effective strategy for inhibition that may be applicable to the Ras/Rac/Rho family of GTPases and their respective guanine nucleotide exchange factors. It would now seem advantageous to conduct *in vitro* drug screening assays with both the GTPase and its GEF and to pursue lead compounds falling in the uncompetitive inhibitor category.

We thank R. Kuchta for discussions on data analysis in Fig. 4; T. Hobman for comments on the manuscript; J. Aitchison, A. Franzusoff, T. Hobman, R. Kahn, W. Nickel, and F. Wieland for providing essential reagents; and S. Misra and J. Roote for consultations about the *Drosophila* homologue. This work was supported by the Alberta Heritage Foundation for Medical Research (S.J.M. and P.M.) and the Medical Research Council of Canada (P.M. and S.W.S.).

1. Klausner, R. D., Donaldson, J. G. & Lippincott-Schwartz, J. (1992) *J. Cell Biol.* **116,** 1071–1080.
2. Orci, L., Tagaya, M., Amherdt, M., Perrelet, A., Donaldson, J. G., Lippincott-Schwartz, J., Klausner, R. D. & Rothman, J. E. (1991) *Cell* **64,** 1183–1195.
3. Donaldson, J. G., Finazzi, D. & Klausner, R. D. (1992) *Nature (London)* **360,** 350–352.
4. Helms, J. B. & Rothman, J. E. (1992) *Nature (London)* **360,** 352–354.
5. Randazzo, P. A., Yang, Y. C., Rulka, C. & Kahn, R. A. (1993) *J. Biol. Chem.* **268,** 9555–9563.
6. Beraud-Dufour, S., Robineau, S., Chardin, P., Paris, S., Chabre, M., Cherfils, J. & Antonny, B. (1998) *EMBO J.* **17,** 3651–3659.
7. Goldberg, J. (1998) *Cell* **95,** 237–248.
8. Chardin, P., Paris, S., Antonny, B., Robineau, S., Beraud-Dufour, S., Jackson, C. L. & Chabre, M. (1996) *Nature (London)* **384,** 481–484.
9. Frank, S. R., Hatfield, J. C. & Casanova, J. E. (1998) *Mol. Biol. Cell* **9,** 3133–3146.
10. Monier, S., Chardin, P., Robineau, S. & Goud, B. (1998) *J. Cell Sci.* **111,** 3427–3436.
11. Franco, M., Boretto, J., Robineau, S., Monier, S., Goud, B., Chardin, P. & Chavrier, P. (1998) *Proc. Natl. Acad. Sci. USA* **95,** 9926–9931.
12. Morinaga, N., Tsai, S-C., Moss, J. & Vaughan, M. (1996) *Proc. Natl. Acad. Sci. USA* **93,** 12856–12860.
13. Morinaga, N., Moss, J. & Vaughan, M. (1997) *Proc. Natl. Acad. Sci. USA* **94,** 12926–12931.
14. Achstetter, T. A., Franzusoff, A., Field, C. & Schekman, R. (1988) *J. Biol. Chem.* **263,** 11711–11717.
15. Mansour, S. J., Herbrick, J.-A., Scherer, S. W. & Melançon, P. (1998) *Genomics* **54,** 323–327.
16. Peyroche, A., Paris, S. & Jackson, C. L. (1996) *Nature (London)* **384,** 479–481.
17. Frank, S., Upender, S., Hansen, S. H. & Casanova, J. E. (1998) *J. Biol. Chem.* **273,** 23–27.
18. Segel, I. H. (1975) *Enzyme Kinetics* (Wiley, New York), pp. 136–143.
19. Heng, H. H. Q. & Tsui, L.-C. (1993) *Chromosoma* **102,** 325–332.
20. Deloukas, P., Schuler, G. D., Gyapay, G., Beasley, E. M., Soderlund, C., Rodriguez-Tome, P., Hui, L., Matise, T. C., McKusick, K. B., Beckmann, J. S., *et al.* (1998) *Science* **282,** 744–746.
21. Peyroche, A., Antonny, B., Robineau, S., Acker, J., Cherfils, J. & Jackson, C. L. (1999) *Mol. Cell* **3,** 275–285.
22. Sata, M., Donaldson, J. G., Moss, J. & Vaughan, M. (1998) *Proc. Natl. Acad. Sci. USA* **95,** 4204–4208.
23. Jones, S., Jedd, G., Kahn, R., Franzusoff, A. & Segev, N. (1999) *Genetics*, in press.
24. Yan, J.-P., Colon, M. E., Beebe, L. A. & Melançon, P. (1994) *J. Cell Biol.* **126,** 65–75.
25. Torii, S., Banno, T., Watanabe, T., Ikehara, Y., Murakami, K. & Nakayama, K. (1995) *J. Biol. Chem.* **270,** 11574–11580.
26. Presley, J. F., Cole, N. B., Schroer, T. A., Hirschberg, K., Zaal, K. J. & Lippincott-Schwartz, J. L. (1997) *Nature (London)* **389,** 81–85.
27. Lowe, M. & Kreis, T. E. (1998) *Biochim. Biophys. Acta* **1404,** 53–66.